Transmission of motor signals from the basal ganglia to the thalamus: effect of correlations, sensory responses, and excitation

Short title: Transmission of basal ganglia motor signals to thalamus

Mohammadreza Mohagheghi Nejad[1,2*], Stefan Rotter[1], Robert Schmidt[3]

1 Bernstein Center Freiburg & Faculty of Biology, University of Freiburg, Freiburg, Germany
2 Department of Computational Science and Technology, School of Electrical Engineering and Computer Science, KTH Royal Institute of Technology, Stockholm, Sweden
3 Department of Psychology, University of Sheffield, Sheffield, United Kingdom

* mohammadreza.mohagheghi@bcf.uni-freiburg.de

Abstract

Basal ganglia output neurons transmit motor signals by decreasing their firing rate during movement. This decrease can lead to post-inhibitory rebound spikes in thalamocortical neurons in motor thalamus (Mthal). While in healthy animals neural activity in the basal ganglia is markedly uncorrelated, in Parkinson's disease neural activity becomes pathologically correlated. Here we investigated the impact of correlations in the basal ganglia output on the transmission of motor signals to Mthal using a Hodgkin-Huxley model of a thalamocortical neuron. We found that correlations in the basal ganglia output disrupt the transmission of motor signals via rebound spikes by increasing the signal-to-noise ratio and trial-to-trial variability. We further examined the role of brief sensory responses in basal ganglia output neurons and the effect of cortical excitation of Mthal in modulating rebound spiking. Interestingly, both the sensory responses and cortical inputs could either promote or suppress the generation of rebound spikes depending on their timing relative to the motor signal. Finally, in the model rebound spiking occurred despite the presence of moderate levels of excitation, indicating that rebound spiking might be feasible in a parameter regime relevant also in vivo. Overall, our model provides novel insights into the transmission of motor signals from the basal ganglia to Mthal by suggesting new functional roles for active decorrelation and sensory responses in the basal ganglia, as well as cortical excitation of Mthal.

Author summary

The output of the basal ganglia might act like a brake on our brain's motor circuits such as motor thalamus. When we move, this brake is released, letting motor thalamus execute the selected movement. However, the neural processes that underlie the communication of the basal ganglia with the motor thalamus during movement are unclear. We utilise a computational model of a neuron in motor thalamus to investigate how this transmission might work, how it can be modulated by sensory and cortical inputs, and how it is compromised in Parkinson's disease. Our results explain how pathological correlations in the neural activity in Parkinson's disease disturb the transmission of motor signals, which might underlie some of the motor symptoms.

Introduction

The basal ganglia (BG) have long been implicated in the selection and execution of voluntary movements [1–4]. Classic "box-and-arrow" models of the BG [5,6] presume a propagation of motor signals through the so-called direct pathway. Increased activity in the striatum, the input region of the BG, reduces the activity in BG output regions (e.g. substantia nigra pars reticulata, SNr), which in turn disinhibits the motor thalamus (Mthal) [7], and thereby enables movement. BG output neurons often have high baseline firing rates and decrease their rate during movement in both rodents and primates [8–11]. However, recent studies have suggested a more complex picture on how BG output affects Mthal and motor cortex [12,13].

Three different modes have been proposed for how the BG output can affect thalamic targets [13]. In the first mode sudden pauses in BG inhibition of thalamus lead to "rebound" spikes, which have been described in thalamocortical neurons in the thalamus due to their intrinsic T-type Ca^{2+} channels [14]. Release from long-lasting hyperpolarisation (e.g. during movement) de-inactivates the T-type Ca^{2+} channels and depolarises the membrane potential. For strong enough preceding hyperpolarisation, the

membrane potential can even reach the spike threshold without any excitation [15–18]. However, thalamocortical neurons also receive excitatory input from cortex, which can affect the transmission mode. In the "disinhibition" mode the BG inhibition can gate cortical excitation so that during pauses of inhibition the excitatory inputs can evoke spikes in the thalamocortical neuron [19–21]. If these excitatory inputs are strong enough, the thalamocortical neuron fires also during the presence of inhibitory inputs with fixed short latency after the inhibitory input spikes from SNr [22, 23].

One prominent feature of the BG network is that neurons fire in an uncorrelated fashion, despite the overlapping dendritic fields and local recurrent connections [24]. Specific features of the BG such as pacemaking neurons and high firing rate heterogeneity may act as mechanisms for active decorrelation of activity. This effectively prevents correlations among neurons, and a disruption of this mechanism leads to pathologically correlated activity as in Parkinson's disease [25]. Increased correlated activity has also been observed in BG output neurons in Parkinson's disease [26], which may compromise the transmission of motor signals. Currently, however, we do not know whether active decorrelation serves a function in BG output and whether this function is compromised in Parkinson's disease.

In addition to transmitting motor signals, BG output neurons may also be involved in further sensory and cognitive processing. For example, SNr neurons also respond to salient sensory stimuli instructing the initiation or stopping of movements [11, 27]. However, how these sensory responses affect thalamic motor circuits remains unclear.

In the present study we used computational modelling to study the information transmission from the BG to the thalamus via postinhibitory rebound spikes. We found that uncorrelated BG output ensures a clear transmission of motor commands with low trial-to-trial variability in the thalamic response latency. In contrast, pathological correlations in SNr lead to a noisy transmission with high trial-to-trial variability. In addition, we found that sensory responses in SNr can, depending on their timing relative to the movement-related decrease, either facilitate or suppress rebound spikes leading to promote or suppress movement. Therefore, in the rebound transmission mode, uncorrelated activity and sensory responses in the BG output serve functional roles in the coordinated transmission of motor signals. Finally, we found that the rebound spiking mode persisted in the presence of excitation, strong enough to maintain baseline firing rates reported in vivo [20].

Materials and methods

Model neuron

In this study we used a Hodgkin-Huxley type model of a thalamocortical neuron [28]. The model has four different ionic currents: a leak current (I_L), a Na^+ current (I_{Na}), a K^+ current (I_K), and a T-type Ca^{2+} current (I_T), which are determined by the membrane potential and the channel conductances and reversal potentials (E). While the conductance of the leak current (g^{max}) is constant, the conductance for Na^+, K^+ and T-type Ca^{2+} currents depends on the membrane potential and varies over time. These voltage-dependent conductances are formed by the product of maximum channel conductance (g^{max}) and voltage-dependent (in)activation variables (m, h, p and r).

The model neuron's membrane potential is described by

$$C_m \frac{dv}{dt} + I_L + I_{Na} + I_K + I_T + I_{SNr\to TC} + I_{CX\to TC} = 0 \quad (1)$$

with a leak current $I_L = g_L^{max}[v - E_L]$. The Na^+ current $I_{Na} = g_{Na}^{max} m_\infty^3(v) h[v - E_{Na}]$ has an instantaneous activation gating variable $m_\infty(v) = \frac{1}{1+exp(-(v+37)/7)}$ and a slow

inactivation gating variable h with $\frac{dh}{dt} = \frac{h_\infty(v)-h}{\tau_h(v)}$ and steady-state $h_\infty(v) = \frac{1}{1+exp((v+41/4))}$ that is approached with a time constant $\tau_h(v) = \frac{1}{a_h(v)+b_h(v)}$; $a_h(v) = 0.128exp(-(v+46)/18)$; $b_h(v) = \frac{4}{1+exp(-(v+84)/4)}$.

The activation variable in K^+ current $I_K = g_K^{max}[0.75(1-h)^4][v-E_K]$ is described in analogy to Na^+ inactivation variable (h) which reduces the dimensionality of the model by one differential equation [29].

The T-type Ca^{2+} channel $I_T = g_T^{max} p_\infty^2(v) r[v-E_T]$ has an instantaneous activation $p_\infty(v) = \frac{1}{1+exp(-(v+60)/6.2)}$ and slow inactivation $\frac{dr}{dt} = \frac{r_\infty(v)-r}{\tau_r(v)}$ with the steady-state $r_\infty(v) = \frac{1}{1+exp((v+84)/4)}$ and time constant $\tau_r(v) = 28 + 0.3(-(v+25)/10.5)$.

The T-type Ca^{2+} channel can cause post-inhibitory rebound spikes by the following mechanism. Prolonged hyperpolarisation leads to de-inactivation of the T-type Ca^{2+} channel, i.e. the inactivation gate (r) opens while the activation gate (p) closes. After shutting down the hyperpolarisation, the inactivation gate closes slowly whereas the activation gate opens very fast. Therefore, while both gates are open, the T-type Ca^{2+} channel briefly opens leading to membrane depolarisation. Strong enough depolarisation can lead to Na^+ spikes which are referred to as post-inhibitory rebound spikes.

The thalamic model neuron receives two types of synaptic inputs; one inhibitory from BG output ($SNr \rightarrow TC$) and one excitatory from cortex ($CX \rightarrow TC$). Synaptic currents (I_X) are described by a simple exponential decay with the decay rate β_X, where X denotes the synapse type [30]. Similar to the intrinsic ionic currents, each synaptic current is described in terms of membrane potential and channel conductance (g^{max}) and reversal potential (v_X): $I_X = g_X^{max}[v-v_X]\sum_j s_j$;
$X = \{SNr \rightarrow TC, CX \rightarrow TC\}$. When a presynaptic neuron j spikes at time t_i, s_j becomes 1 and decays with time constant β afterwards $\frac{ds_j}{dt} = (1-s_j)\delta(t-t_i) - \beta_X s_j$, where $\delta(t)$ is the Dirac delta function. The maximum conductance caused by a single presynaptic spike ($s_j = 1$) is represented as g_X^{max}. The net synaptic current is the summation of all presynaptic events s_j multiplied by the difference of the membrane potential and synaptic reversal potential. Therefore, the reversal potential can change the synaptic current. The inhibitory reversal potential used in this model ($v_{SNr\rightarrow TC} = -85mV$) with $g_{SNr\rightarrow TC} \approx 1.2nS/\mu m^2$ can reproduce the inhibitory current ($\sim 100\ pA$ when membrane potential is held at 0 mV for minimal stimulation intensity) reported in vitro [31]. The intrinsic and synaptic parameters of the model neuron are described in Table 1.

Table 1. Model parameters: intrinsic, inhibitory synapses [28] and excitatory synapses [32].

$g_L = 0.05\ nS/\mu m^2$	$E_L = -70\ mV$	$g_{Na} = 3\ nS/\mu m^2$	$E_{Na} = 50\ mV$
$g_T = 5\ nS/\mu m^2$	$E_T = 0\ mV$	$g_K = 5\ nS/\mu m^2$	$E_K = -90\ mV$
$v_{SNr\rightarrow TC} = -85\ mV$	$\beta_{SNr\rightarrow TC} = 0.08\ ms^{-1}$	$v_{CX\rightarrow TC} = 0\ mV$	$\beta_{CX\rightarrow TC} = 0.18\ ms^{-1}$

g: Ionic channel conductance; E: ionic channel reversal potential; v: synaptic reversal potential; β: decay rate of synaptic current.

Input spike trains

We generated uncorrelated and correlated Poisson spike trains as inputs to the model neuron. To generate uncorrelated spike trains we simulated N independent Poisson processes, each with the firing rate r. To quantify correlation in spike trains, we used the average pairwise correlation among them, denoted by ϵ. However, for $N \geq 3$ and a pairwise correlation of ϵ_0, different realisations of spike trains with different correlations of order 3 or higher are possible. For a convenient parametrisation of the order of correlation, we used the distribution of coincident spikes ("amplitude", A) in a model of

interacting Poisson processes [33]. For a homogeneous population of spike trains, the average pairwise correlation depends on the first two moments of the random amplitude A:

$$\epsilon = \frac{\frac{E[A^2]}{E[A]} - 1}{N - 1} \tag{2}$$

One can consider different amplitude distributions for Poisson spike trains with a given rate r and pairwise correlation ϵ. In the present study, we specifically used binomial and exponential amplitude distributions (Figure 1). While the binomial amplitude distribution has a high probability density around the mean of the distribution (Figure 1A), the exponential distribution has a higher probability density toward lower amplitudes [34] (Figure 1B).

To generate spike trains with a binomial amplitude distribution we implemented a multiple interaction process [35] (Figure 1A). For correlated outputs ($\epsilon > 0$), the algorithm starts from a Poisson spike train with rate λ, the so called "mother" spike train. We derived neuronal spike trains by randomly and independently copying spikes of the "mother" spike train with probability ϵ, leading to spike trains of rate $r = \epsilon\lambda$.

We also generated spike trains using exponentially distributed amplitudes described by:

$$f_A(\xi;\tau) = \frac{e^{-\tau\xi}}{\sum_{k=1}^{N} e^{-\tau k}}; \xi \in [1,\ N] \tag{3}$$

where $f(\xi;\tau)$ is the probability density for each amplitude ξ with the parameter τ. According to Eq. 2, to compute ϵ for this distribution, we needed to compute the proportion of the second moment to the first moment for this distribution. We used $E[A^n] = \sum_{\xi=1}^{N} \xi^n f_A(\xi)$ to compute the first and second moments of the distribution and then applied it into Eq. 2, rewriting it to

$$\epsilon = \frac{\sum_{\xi=1}^{N} \frac{\xi^2 e^{-\tau\xi}}{\xi e^{-\tau\xi}} - 1}{N - 1} \tag{4}$$

This equation shows that ϵ depends on τ and we took a simple numerical approach to find τ for each desired ϵ. We computed ϵ for a range of τ (from 0 to 5 with steps of 0.001) and then selected the τ that yielded an ϵ closest to our desired ϵ (Figure 1C). The maximum error between the ϵ we calculated using Eq. 4 and the desired ϵ was 5×10^{-4}.

The next step was to generate the population spike trains using the probability distribution determined by the τ we already computed. We drew N independent Poisson spike trains each with rate $r_\xi = Nrf_A(\xi)/\xi$; $\xi \in [1,\ N]$. Since ξ represents the number of coincident spikes in a time bin, spike times from independent spike trains should be copied ξ times to get the final population spike train. As the amplitude distribution described in Eq. 3 has a high probability density toward lower amplitudes, high average pairwise correlations cannot be achieved. For typical parameters of the inhibitory input spike trains in this study ($N = 30$, $r = 50Hz$), the maximum average pairwise correlation was 0.65 for $\tau = 0$ (Figure 1C). The number of SNr neurons projecting to the same Mthal neuron is currently not known. However, current estimates based on optogenetic stimulation of nigral terminals in the ventromedial thalamus in mouse brain slices suggest that there might be more than 20 different inputs from SNr [21]. In our model, each inhibitory input spike lead to an inhibitory post-synaptic potential (IPSP) with amplitude 1 mV under $g_{SNr\to TC} = 1nS/\mu m^2$. Since the hyperpolarisation caused by inhibition cannot go below -85mV due the inhibitory reversal potential, 18 synchronous inhibitory inputs exerted the maximal hyperpolarisation from the resting potential to -85mV (-85mV - (-67mV) = -18mV corresponding to 18 IPSPs). As a

consequence, although we did all simulations throughout this study using 30 inhibitory inputs, similar results would be achieved with fewer inputs, too.

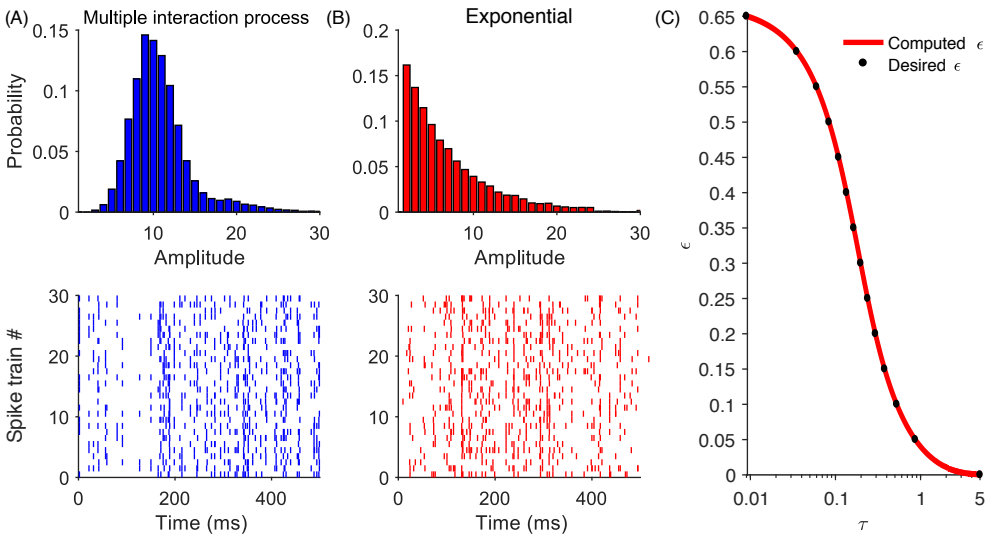

Fig 1. Generation of correlated Poisson spike trains used as input to the model neuron. (A, top) Amplitude distribution of the higher-order correlations in spike trains generated by the multiple interaction process with with $\epsilon = 0.3$ and $r = 50\ Hz$. Bottom panel shows the raster plot of 30 respective example spike trains. (B, top) Amplitude distribution of higher-order correlations in spike trains generated by an exponential amplitude distribution with $\epsilon = 0.3$ and $r = 50\ Hz$, and corresponding example spike trains (bottom panel). (C) Relation between the parameter τ of an exponential amplitude distribution and the resulting average pairwise correlation ϵ (red trace). Black dots represent the average pairwise correlations that we used to generate input spike trains with exponential amplitude distribution.

Data analysis

Identifying rebound spikes

The model neuron can spike in response to excitatory input or due to release from inhibition with post-inhibitory rebound spikes. To distinguish "normal" spikes driven by excitatory inputs from post-inhibitory rebound spikes, we repeated simulations with exactly the same input (identical seed for the random number generator), but with a modified model that is unable to create rebound spikes. Post-inhibitory rebound spikes are due to the de-inactivation of T-type Ca^{2+} channels, so without this channel rebound spikes cannot occur. Therefore, we classified spikes as rebound spikes, if they disappeared after the removal of T-type Ca^{2+} channels (i.e. $g_T = 0\ nS/\mu m^2$). However, to reduce potentially confounding effects, we ensured that the overall spiking behaviour remained similar by increasing the Na^+ channel conductance to $g_{Na} = 6\ nS/\mu m^2$.

Due to the randomness of the inhibitory input spike trains, the generation of a rebound spike was probabilistic. This was in particular prominent in simulations with weak inhibition (see e.g. Figure 6A). Therefore, we measured the effect of sensory responses (Figure 4) and single excitatory spikes (Figure 5) by the change in the probability of rebound spikes.

In the simulations in which we investigated the effect of ongoing excitation, we observed that for some parameters rebound and disinhibition modes overlapped. To

characterise this concurrence, we computed the firing rate in a scenario with only inhibitory inputs to achieve the time interval where rebound spikes occured. Then we ran the same simulation again, but this time with only ongoing excitation, and again computed the firing rate in the same interval. Finally, we ran the simulation in a scenario including both inhibitory and excitatory inputs, and again computed the firing rate in this interval. We then subtracted the firing rate of the excitation-only simulation from the firing rate from the simulation with both inhibitory and excitatory input. The resulting firing rate difference indicated the contribution of the rebound activity. We compared this rate difference with the rate we computed in the scenario with only inhibitory inputs to compute the proportion of trials in rebound mode.

Transmission quality

For our simulations shown in Figure 2, we needed to quantify the transmission quality for a variety of inputs strengths and degrees of correlation. For a clear transmission of the motor signal the thalamocortical neuron would ideally respond only to the movement-related decrease of activity in SNr neurons with a rebound spike, and be silent otherwise. Any rebound spike before the movement-related decrease would make the transmission noisy, in the sense that the decoding of the presence and timing of the motor signal in thalamic activity would be less accurate. Therefore, we used the number of spikes after the onset of the movement-related decrease, normalised by the total number of spikes within -1 s to 0.5 s around the onset of the movement-related decrease as a measure of the transmission quality.

Software packages

We implemented the model neuron in Simulink, a simulation package in MATLAB (R2016b) and used a 4th-order Runge-Kutta method to numerically solve the differential equations (time step = 0.01 ms). We wrote all scripts to generate input spike trains, handle simulations and analyse and visualise the simulation data in MATLAB. To run the simulations we used the "NEMO" high-performance computing cluster in the state of Baden-Wuerttemberg (bwHPC) in Germany.

Data availability

We provided our simulation scripts (in "BasicModelSimulations" directory) including the scripts generating input spike trains (in "SpikeTrains" directory) accessible via a git repository `https://github.com/mmohaghegh/NigrothalamicTransmission.git`

Results

Uncorrelated activity promotes transmission of motor signals

To determine whether uncorrelated activity in BG output is important for the transmission of motor signals, we simulated a thalamocortical neuron exposed to inhibitory Poisson input spike trains with varying degrees of correlation (Figure 2). We used binomial and exponential amplitude distributions to generate correlated Poisson spike trains (see Materials and Methods). In addition, we modulated the input firing rate so that it mimicked the prominent movement-related decrease of BG output neurons observed in experimental studies [8–11].

For uncorrelated inputs the model responded to the movement-related decrease with a single rebound spike (Figure 2A, left panel). However, for correlated inputs rebound spikes appeared not only after the movement-related decrease, but also at random times

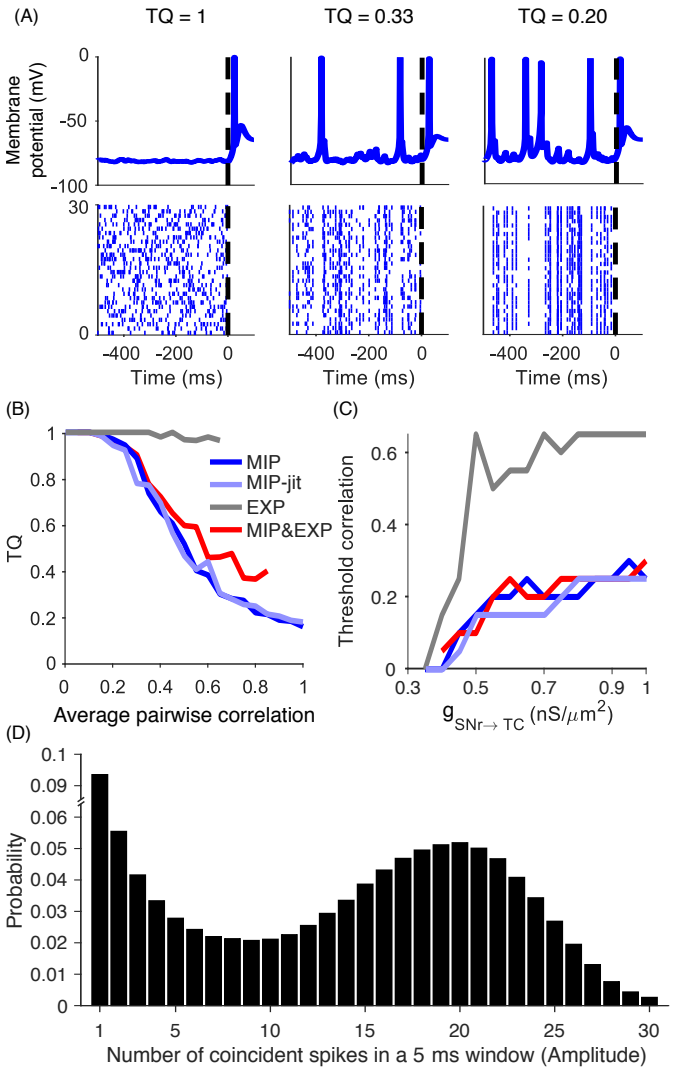

Fig 2. Input spike correlations impair transmission quality (TQ) of motor signals from SNr to thalamus. (A) Top panels show the intracellular response of the thalamocortical model neuron to the inhibitory input spike trains from SNr displayed in the bottom panel. Uncorrelated Poisson spike trains ($\epsilon = 0$) lead to clear transmission via a single rebound spike after the firing rate decrease in the input (left panel). Correlated Poisson spike trains, however, lead to rebound spikes at random times, whenever there is a pause in the input spike trains (middle panel: $\epsilon = 0.35$ and right panel: $\epsilon = 0.7$). (B) TQ drastically decreases for correlated input spike trains generated according to the multiple interaction process (MIP; dark blue). This holds also for the multiple interaction process whose synchroneous spike times are jittered in a 5 ms window (MIP-jit; light blue). Data shown is an average of 100 trials with $G_{SNr\rightarrow TC} = 0.70\ nS/\mu m^2$. TQ only slightly decreases for the spike trains generated by exponential amplitude distributions (EXP; grey), which is dominated by lower-order instead of higher-order correlations. Note that the exponential amplitude distribution leads to the maximum average pairwise correlation of 0.65 (see Materials and Methods). The black dot marks the TQ for the spike trains generated using the amplitude distribution shown in (D). For amplitude distributions with binomial and exponential components of similar proportion (D), TQ decreases drastically for correlated inputs (MIP&EXP; red). (C) Threshold correlation at which the transmission quality deteriorates ($TQ < 0.95$) only weakly depends on the inhibitory input strength. For the scenarios involving higher-order correlations (blue and red lines), already weak correlations are sufficient to deteriorate transmission. (D) The simulation of Parkinson's disease in a large-scale model of the BG yielded an amplitude distribution of SNr spike times that corresponded to a mixture of the exponential and binomial amplitude distributions.

during baseline activity (Figure 2A, middle and right panels). The reason for this was that correlated SNr activity lead not only to epochs with many synchronous spikes, but also to pauses in the population activity that were long enough to trigger rebound spikes.

In mammals multiple inhibitory projections from SNr converge on a single thalamocortical neuron [21], which affects the strength of the inhibition on the thalamocortical neuron. Since the degree of convergence is not clear, we repeated our simulations for different inhibitory strengths, but found that the transmission quality did not depend on the inhibitory strength as long as the inhibition was strong enough to lead to rebound spikes (Figure 2C). Furthermore, as for more than two inputs the input spike trains cannot be uniquely characterised by pairwise correlations, we considered two different possibilities for higher-order correlations (see Materials and Methods). We found that the transmission quality strongly depended on both the input average pairwise correlation and higher-order correlations among input spike trains (Figure 2B).

Pairwise correlations affected the transmission only for a binomial amplitude distribution (Figure 2B, dark blue trace), but not for an exponential amplitude distribution (Figure 2B, grey trace). For the binomial amplitude distribution higher-order events ("population bursts") are common, which increases the probability for pauses in the population activity. Thereby, even weak correlations among SNr spike trains lead to a sharp decrease in the transmission quality. In contrast, for spike train correlations with an exponential amplitude distribution, the decrease in transmission quality was less pronounced (Figure 2B, grey trace). This was because for the exponential amplitude distribution lower-order events are more common, which are not sufficient for pauses in the population activity of SNr neurons leading to thalamic rebound spikes. Therefore, in particular higher-order correlations may be detrimental for the transmission of motor commands.

We further investigated whether the sharp decrease in the transmission quality observed for the binomial amplitude distribution was due the perfect synchrony of correlated spike times. So we jittered the synchronous events by randomly displacing individual spikes by up to 5ms (2B, light blue trace). We found a similar transmission quality (2B, light blue trace vs. dark blue trace) confirming that the sharp decrease was not due to the perfect synchrony.

The purpose of our simulation of correlated activity was to mimic BG output patterns in Parkinson's disease. However, as the amplitude distribution of pathologically correlated activity in SNr is currently unknown, we employed a large-scale model of the BG [36], in which beta oscillations propagate through cortico-basal ganglia circuits. Beta oscillations are widely observed in animals with dopamine-depleted basal ganglia including their output nuclei [37, 38]. While beta oscillations can be generated in the pallido-subthalamic loop [39], here we do not assume a specific mechanism for the generation of correlated activity in Parkinson's disease, but focussed on the amplitude distribution in SNr in a simulation of Parkinson's disease. We found that the amplitude distributions in the dopamine-depleted state of the large-scale model were somewhere between binomial and exponential (Figure 2D). Therefore, to investigate the model with a correlation structure that might be relevant for Parkinson's disease, we generated input spike trains based on this distribution (see Materials and Methods). We found that this input led to a low transmission quality (Figure 2B, black dot). In addition, we investigated the effect of average pairwise correlation, if the amplitude distribution was a mixture of binomial and exponential distributions. To achieve this, we changed the pairwise correlation for the binomial component of the distribution, while keeping the pairwise correlation for the exponential component unchanged (Figure 2B, red trace). In this mixed distribution we found that changing only the pairwise correlation of the binomial component had a similar effect on the transmission quality as in the standard

binomial amplitude distribution (Figure 2B, red and blue traces). This confirms that under a correlation structure similar to Parkinson's disease, even weak correlations in BG output can impair the transmission of motor signals, potentially related to motor symptoms such as tremor or akinesia [18, 21, 40].

Uncorrelated activity enhances transmission speed

To study the effect of input correlations on transmission speed, we used the same scenario as above (Figure 2) and measured the time between the onset of the movement-related decrease and the rebound spike. We found that for no or weak correlations the transmission speed was fast, but it decreased for stronger correlations (Figure 3A). Therefore, uncorrelated activity in BG output regions may also promote fast transmission of motor signals. To generalise our findings on the transmission speed beyond the scenario using the movement-related decrease, we further examined transmission speed using (rebound) spike-triggered averages of inputs. Instead of simulating a movement-related decrease, we exposed the model neuron to inhibitory inputs with a constant firing rate. To compute the spike-triggered average, we used the peak of each rebound spike as the reference time point to compute the average of the preceding input. Since rebound spikes occurred more often for stronger input correlations, we performed this analysis on inputs having a correlation coefficient of either 0.3 or 1.0. These simulations confirmed that weak input correlations induce faster transmission than strong correlations (Figure 3C).

Uncorrelated activity enhances transmission precision

For the transmission of motor signals via rebound spikes the trial-to-trial variability of the transmission may be important. For example, for the coordination of motor signals across different neural pathways a small variability (i.e. high precision) of the transmission speed might be important. To investigate the nigrothalamic transmission variability, we computed the variance over the latencies across 100 trials with movement-related decreases in SNr activity (i.e. the same scenario as in Figure 3A). We found that for uncorrelated inputs transmission was very precise in the sense that the trial-to-trial variability of the response latency was small (Figure 3B). In contrast, even weak correlations led to a high transmission variability due to changes in the amount of hyperpolarisation caused by correlated inputs preceding rebound spikes. We conclude that uncorrelated inputs ensure a high precision of the transmission via rebound spikes by reducing the trial-to-trial variability in response latency.

Sensory responses can promote or suppress rebound spiking

SNr neurons often have short-latency responses to salient sensory stimuli characterised by brief increases in firing rate [27]. In rats performing a stop-signal task these responses also occurred in neurons that decreased their activity during movement [11]. This included responses to auditory stimuli, which cued the initiation of a movement (Go cue) or the cancellation of an upcoming movement (Stop cue). We examined how such brief increases in SNr activity affect rebound spiking in the thalamocortical model neuron (Figure 4). The thalamocortical model neuron received inputs similar to the SNr firing patterns recorded in rats during movement initiation (i.e. uncorrelated inputs with high baseline firing rate and a sudden movement-related decrease). To model sensory responses in the SNr neurons, we added a brief increase in firing rate at different time points relative to the movement-related decrease (Figure 4A). We generated the brief increase by adding a single spike in each spike train having the

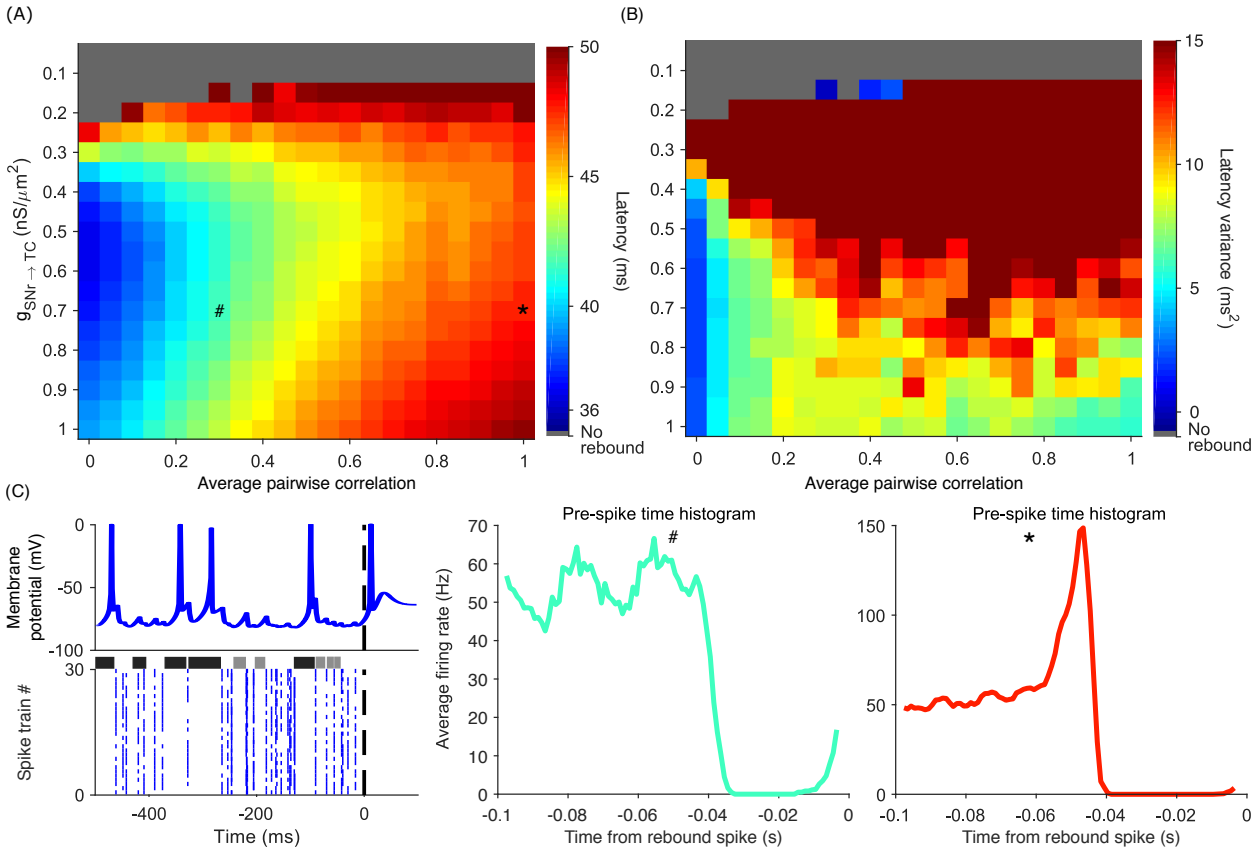

Fig 3. Correlated SNr spike trains decrease transmission speed and temporal precision of rebound spikes. Systematic investigation of average transmission latency (A) and its variance (B) for different degrees of correlation and inhibitory strengths identifies the range with fastest transmission speed and highest transmission precision, respectively. (C) Left panel shows a sample membrane potential ($G_{SNr\to TC} = 0.70\ nS/\mu m^2$, $\epsilon = 0.7$; top) of the thalamocortical model neuron and the corresponding inhibitory inputs (bottom). Note that rebound spikes are preceded by pauses in the input raster plot (indicated by black horizontal bars). However, for very short pauses (indicated by grey horizontal bars) no rebound spikes occur. (C) Averages triggered by rebound spikes for weakly correlated inputs (middle panel) and strongly correlated inputs (right panel) confirm that pauses in the inhibitory input precede rebound spikes. The duration of the pause preceding the rebound spikes indicates the transmission latency. The inset symbols in (A) indicate the parameters used for the corresponding spike-triggered averages in (C).

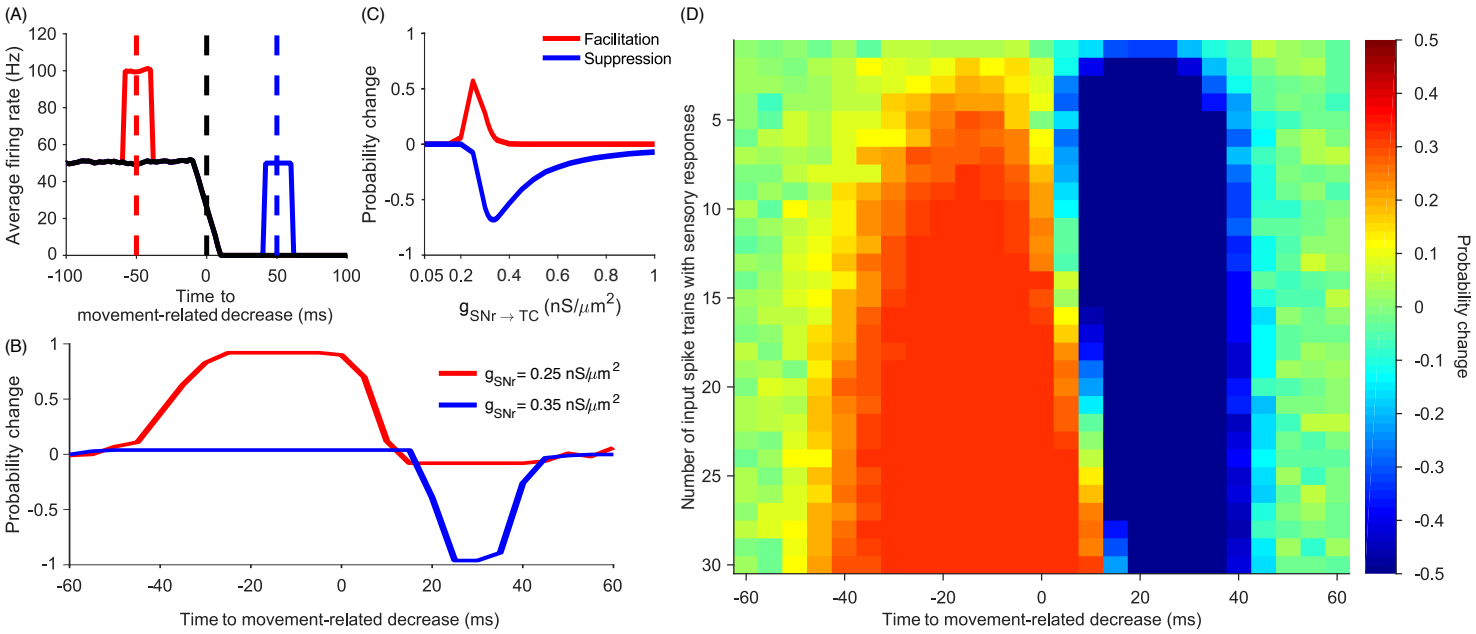

Fig 4. Sensory responses simulated as phasic increases in SNr firing rate change the probability of rebound spikes in the thalamocortical model neuron. (A) Average firing rate of example inputs used for simulation experiments. Black solid line shows the inputs average firing rate without sensory responses. Colored solid lines shows the average firing rate with sensory responses in blue when the increase appears after the decrease and in red when the increase appears before the decrease. (B) Changes in the probability of a rebound spike for two different inhibitory input strengths. For the simulation scenario with the inhibitory input strength shown in red, the large probability change indicates that the sensory responses not only facilitated rebound spikes, but they were actually required for their generation. In contrast, for the simulation scenario shown in blue, precisely timed sensory responses almost completely suppressed rebound spikes. (C) Average changes in the probability of rebound spike generation against different inhibitory input strengths. The average is computed over all inputs with sensory responses in a specific time interval (for facilitation from -30 ms to 0 ms and for suppression from 10 ms to 30 ms). (D) Systematic investigation of the effect of sensory responses in a parameter regime, in which the suppression and facilitation of rebound spikes was possible ($G_{SNr \rightarrow TC} = 0.30\ nS/\mu m^2$). Note the large impact of the timing of the sensory response, even if it occurs only in a small subset of neurons, on the probability of rebound spikes.

sensory response at the desired time point. This allowed us to observe the effect of the timing of sensory responses on rebound spiking.

To quantify the effect of sensory responses, we measured the difference in the probability of generating a rebound spike after the movement-related decrease in simulations with and without sensory responses. Interestingly, the sensory responses could either increase or decrease the probability of generating a rebound spike, depending on their relative timing to the movement-related decrease (Figure 4B, D). For sensory responses preceding the movement-related decrease for up to 40 ms, the probability of generating a rebound spike was increased. This was because the sensory response lead to additional hyperpolarisation in the thalamocortical neuron, which promoted rebound spiking. In contrast, for sensory responses occurring 10-40 ms after the movement-related decrease, the probability of generating a rebound spike was decreased. This was because the sensory response in that case partly prevented the movement-related pause of SNr firing. Together, this points to the intriguing possibility that sensory responses in SNr can have opposite effects on behaviour (either promoting or suppressing movement), depending on their timing (Figure 4D). This could explain why SNr neurons respond to both Go and Stop cues with a similar increase in firing

rate [11, 41], a previously puzzling finding (see Discussion).

In addition to the timing of sensory responses relative to the movement-related decrease, also the inhibitory input strength modulated the probability of generating a rebound spike (Figure 4). For weaker inhibitory inputs ($G_{SNr\to TC} = 0.25nS/\mu m^2$), the probability of generating a rebound spike was increased because the additional inhibitory inputs contributed to the hyperpolarisation of the thalamocortical neuron. However, for slightly stronger inputs ($G_{SNr\to TC} \geq 0.35nS/\mu m^2$), the sensory responses could not further facilitate rebound spiking because the probability of generating a rebound spike was already one. Accordingly, sensory responses were most effective in reducing the probability of generating a rebound spike for medium input strengths (i.e. with a relatively high probability of generating a rebound spike). We found that the most effective strength for suppressing rebound spikes was at $G_{SNr\to TC} = 0.35nS/\mu m^2$. However, the suppressing effect vanished for $G_{SNr\to TC} \geq 0.8nS/\mu m^2$ because for this strength the sensory responses themselves caused a hyperpolarization strong enough to trigger a rebound spike (Figure 4C). Therefore, the effect of sensory responses in SNr on motor signals strongly depended on the nigrothalamic connection strength.

Rebound spikes in the presence of excitation

Having studied basic properties of rebound spiking in the model under somewhat idealised conditions, we next extended the model to account for further conditions relevant in vivo. For example, when studying the response of the thalamocortical neuron to inhibitory SNr inputs, we have assumed so far that the movement-related decrease is present in all inputs. However, this is not the case, and the amplitude of the decrease varies across neurons [11]. Therefore, we investigated the response of the thalamocortical model neuron in a scenario in which only a fraction of SNr inputs decreases their firing rates, while the remaining neurons do not change their rates (Figure 5). We found that the thalamocortical model neuron elicits a rebound spike with high probability only when a large fraction of input neurons decrease their firing rates to zero (Figure 5A).

The large fraction of SNr neurons required to exhibit a movement-related decrease in order to elicit a rebound spike downstream constrains the scenario under which this transmission is plausible in vivo. However, in a more realistic scenario the thalamocortical neuron also receives excitatory inputs (e.g. from cortex). Therefore, we examined whether excitatory input can, under some conditions, enhance the transmission via rebound spiking (Figure 5B-D). Importantly, the excitatory inputs should be weak enough in order not to elicit spikes themselves. We simulated the model neuron by adding a single excitatory input spike with variable timing with respect to the movement-related decrease in the inhibitory inputs, and observed whether it promoted or suppressed rebound spikes. We investigated the effect of the excitatory spike on the probability of generating a rebound spike by comparing a simulation including excitatory and inhibitory inputs with a simulation that included only inhibitory inputs. We found that for parameter regions in which the probability of generating a rebound spike was usually small (i.e. in the dark blue region in Figure 5A), additional excitatory spikes after the movement-related decrease increased the rebound probability (Figure 5B). We confirmed that these spikes in the thalamocortical neuron are actually rebound spikes (and not just driven by the excitatory input; see Materials and Methods). However, for strong excitation the thalamocortical model neuron spiked even before the movement-related decrease, indicating that these spikes were no longer rebound spikes.

For parameter regions in which the probability of generating a rebound spike was high (i.e. outside the dark blue region in Figure 5A), the excitatory input spikes could also suppress the generation of rebound spikes when they occurred before the movement-related decrease (Figure 5C). In contrast, when the excitatory input spike occurred after the movement-related decrease, it enhanced the probability of generating

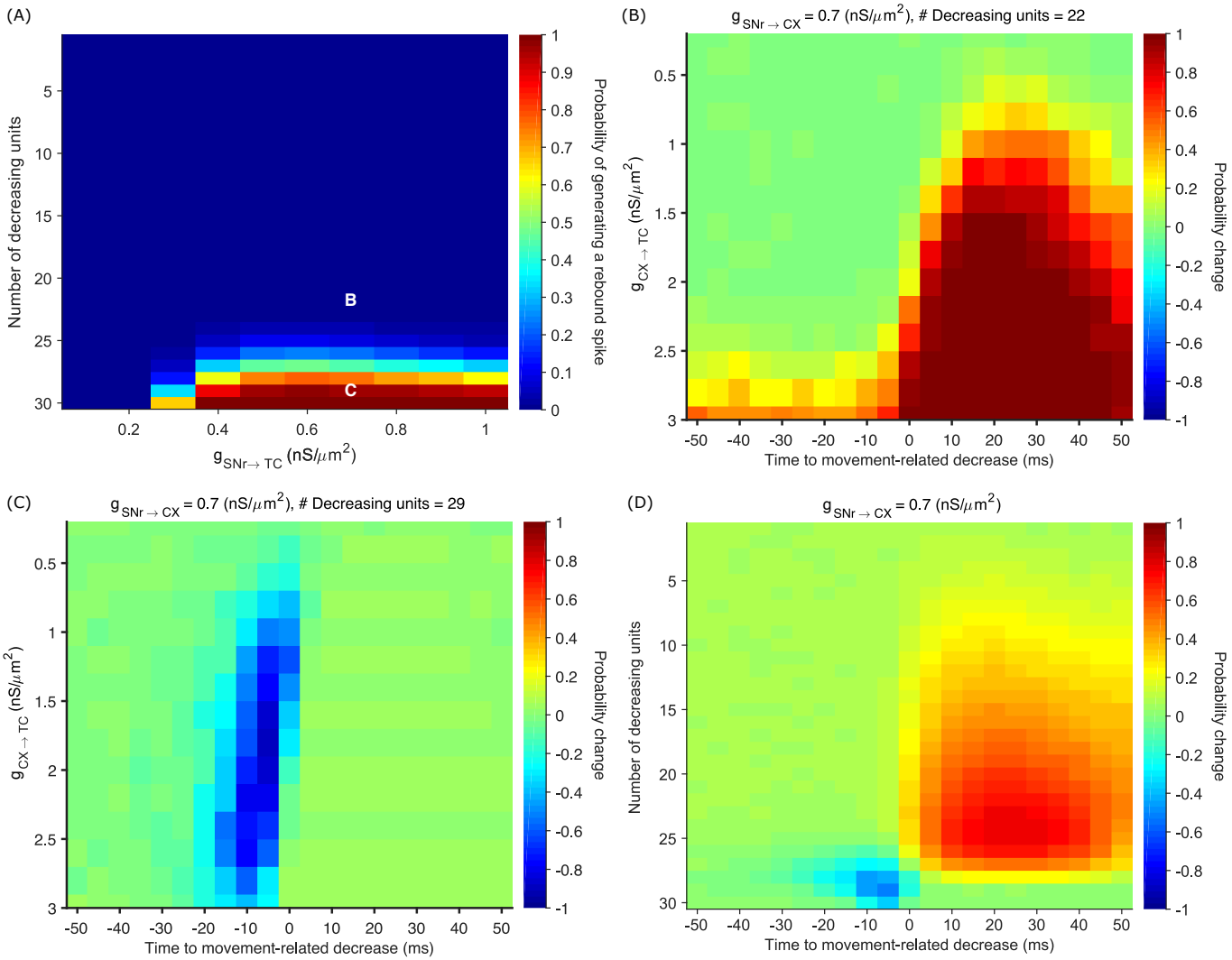

Fig 5. Effect of precisely timed excitatory input spikes on rebound spiking. (A) The generation of rebound spikes requires that a large fraction of the inhibitory input spike trains exhibit a movement-related decrease in firing rate, largely independent of their input strength. (B) Adding a single excitatory spike as input to the thalamocortical model neuron strongly increases the probability of rebound spike generation compared to pure inhibitory inputs (letter "B" in panel A). Note that this occurs in a regime, in which usually no rebound spike can be generated because not enough (here 22 out of 30) neurons decrease their firing rate. (C) In a regime, in which usually rebound spikes are generated (letter "C" in panel A), adding a single excitatory spike as input to the thalamocortical neuron decreases the probability of rebound spike generation compared to pure inhibitory inputs. (D) Systematic investigation of the parameter space indicates a narrow regime, in which a single excitatory spike can decrease, and a larger regime, in which it can increase the probability of a rebound spike. Here, the probability changes are averaged over excitatory input strengths.

a rebound spike. Therefore, similar to the complex effect of sensory responses in SNr neurons described above, also the excitatory input to the thalamocortical neurons could either promote or prevent rebound spikes depending on its timing. Furthermore, if only a fraction of SNr neurons exhibited a movement-related decrease, precisely timed excitatory input could promote the transmission of the motor command to the thalamocortical neuron (Figure 5D). Overall, our simulations indicate that rebound spikes can occur in a broad parameter regime that also includes excitation. Furthermore,

precisely timed excitation provides an additional rich repertoire of rebound spike modulation, either promoting or suppressing movement-related rebound spikes.

Transmission modes revisited: prevalence of rebound spiking

The interaction of excitation and inhibition in thalamocortical neurons is important because even weak excitation may change the transmission mode from rebound to disinhibition [13]. As we observed rebound spiking in the presence of single excitatory spikes (Figure 5), we further investigated how ongoing excitation affects the mode of nigrothalamic transmission. As before, we simulated the model neuron with movement-related inhibitory inputs, but added a background excitation in the form of a Poisson spike train with the firing rate of 100 Hz and examined the effect of changing excitatory strength (Figure 6). In the rebound and disinhibition transmission modes, in an ideal scenario, the model neuron fires spikes exclusively after the movement-related decrease in the firing rate of inhibitory inputs. These spikes are either generated via post-inhibitory rebound spikes in the rebound mode, or via depolarisation through excitation in the disinhibition mode. However, we found that rebound and disinhibition modes can coexist in regimes in which the model neuron has non-zero baseline firing rates (Figure 6A).

We characterised the nigrothalamic transmission mode (see Materials and Methods) according to the proportion of trials with rebound spikes for a range of inhibitory and excitatory inputs strengths (Figure 6A). Motor signals were transmitted via rebound spikes even in the presence of weak excitatory inputs ($G_{CX\rightarrow TC} \leq 1.5\ nS/\mu m^2$; Figure 6A). Interestingly, the transition from rebound to disinhibition mode was not abrupt, but there was a region where disinhibition and rebound spikes coexisted (Figure 6D). In these overlapping regions rebound spiking seemed to be the dominant firing pattern with a strong, transient firing rate increase in response to the movement-related decrease, a phenomenon which was already observed in anesthetised songbirds [19](Figure 6D; see also Discussion). We also examined the effects of varying the firing rate of the excitatory inputs (200, 500, and 1000 Hz). While the rebound and disinhibition spiking mode still overlapped, the corresponding parameter region was shifted towards lower excitatory conductances (not shown). For moderate excitatory input firing rates (100 and 200 Hz), rebound spiking occurred also in regions in which the model neuron was spontaneously active (Figure 6E). This overlap happened for spontaneous activities up to 3 Hz in line with the average spontaneous firing of Mthal neurons in rats during open-field behavior [20]. However, for higher spontaneous activities (>7 Hz) rebound spiking vanished. We conclude that the model neuron can transmit motor signals in the rebound mode despite excitatory inputs.

In summary, our computational model suggests new functional roles for uncorrelated BG output in the clear transmission of motor signals. In addition, the motor signals transmitted via rebound spikes could either be suppressed or promoted through sensory responses indicating that thalamocortical neurons may be a key site for the integration of sensory and motor signals. Finally, excitatory inputs to the thalamocortical neurons do not necessarily prevent rebound spiking, but may as well support the generation of rebound spikes.

Discussion

We used computational modelling to study the impact of spike train correlations in the basal ganglia output on the transmission of motor signals. Based on previous studies [8–11], we focused our description on movement-related pauses in SNr that potentially drive rebound spikes in Mthal. However, as e.g. also neurons in the superior

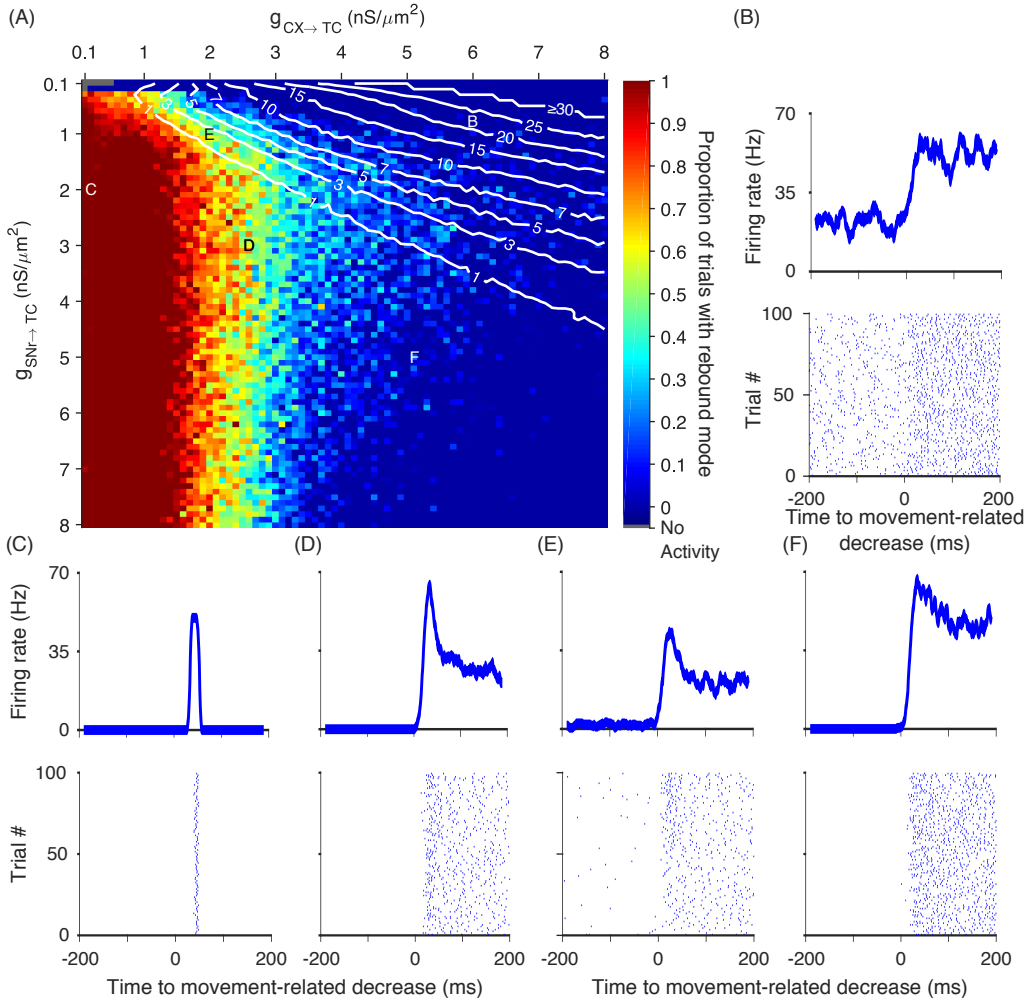

Fig 6. Smooth transition of parameter regimes for rebound and disinhibition transmission modes. (A) The probability of generating a rebound spike (colour-coded) as a function of the strength of the inhibitory and excitatory inputs innervating the thalamocortical neuron indicates the transmission mode. High rebound probability (red) indicates the rebound transmission mode; low rebound probability (blue) indicates the disinhibition transmission mode. Note the gradual transition between transmission modes as a function of the excitatory input strength. The white isolines show the baseline firing rate of the model neuron (i.e. the firing rate before the onset of the movement-related decrease in the input). In the grey region the model neuron does not fire at all. (B-F) Sample firing rate profiles and corresponding raster plots show the activity of the thalamocortical neuron different regions of the transmission map (as indicated by the corresponding letters in A). In the disinhibition mode the neuron fires spontaneously after the decrease in SNr firing rate (F). In the transition regime, rebound and disinhibition modes can coexist (D), and neurons can be spontaneously in the regime with rebound spikes (E).

colliculus can respond with a rebound spike after prolonged hyperpolarisation [42], our modelling results might apply more generally. Furthermore, while previous studies identified the important role of excitation in determining regimes in which rebound spikes can occur [13, 21], our model produced rebound spikes in a wider parameter regime, also in the presence of excitation (Figure 6). In addition, rebound spiking overlapped with the disinhibition transmission mode, indicating that rebound spiking might apply more widely for nigrothalamic communication in line with recent experimental evidence [18]. In our model, the impaired nigrothalamic transmission of motor signals for correlated inputs also indicates a potential functional role of active decorrelation in BG output regions [24].

Functional role of active decorrelation in the basal ganglia

One prominent feature of neural activity in the healthy BG is the absence of spike correlations [25]. This might be due to the autonomous pacemaking activity of neurons in globus pallidus externa/interna (GPe/GPi), subthalamic nucleus (STN) and SNr, as well as other properties of the network such as heterogeneity of firing rates and connectivity that actively counteracts the synchronisation of activity [24]. While uncorrelated BG activity may maximise information transmission [43], our simulations demonstrate that it further prevents the occurrence of random pauses in SNr/GPi activity that could drive thalamic rebound spikes. Thereby, uncorrelated BG output activity may ensure that rebound spikes in Mthal neurons occur only upon appropriate signals such as movement-related decreases in BG output firing rate. In contrast, correlated BG output activity leads to rebound activity in Mthal even at baseline SNr activity, i.e. also in absence of any motor signal. This increase in the signal-to-noise ratio of motor signals may cause problems in motor control.

Evidence for the functional relevance of uncorrelated BG activity originates from the prominent observation that BG activity becomes correlated e.g. in Parkinson's disease [26, 44]. Therefore, our simulations with correlated BG output activity capture a key aspect of neural activity in Parkinson's disease. Interestingly, our finding that BG correlations increase the rate of Mthal rebound spikes is in line with recent experimental findings. In dopamine-depleted mice with Parkinson-like motor symptoms, the rate of Mthal rebound spikes was also increased compared to healthy controls [18]. Furthermore, an increased trial-to-trial variability of rebound spikes was found in dopamine-depleted mice, similar to our simulations (Figure 3).

Therefore, our results support a functional role for active decorrelation in the clear transmission of motor signals with low trial-to-trial variability from the BG to Mthal. Pathological correlations lead to unreliable or noisy transmission of motor signals with high trial-to-trial variability, which may contribute to motor symptoms in Parkinson's disease.

Role of rebound spikes for motor output

In our simulations we only examined the activity of a single thalamocortical neuron. However, for motor signals propagating further downstream, the coordination of activity among different thalamocortical neurons might be relevant. Due to the low trial-to-trial variability of the response latency and the high probability of generating a rebound spike in the model, pauses in population SNr activity would lead to synchronous rebound spikes in different thalamocortical neurons. In contrast, the excitation-driven Poisson-like cortical inputs would not lead to synchronous activity across different thalamocortical neurons. Even though downstream regions cannot directly distinguish thalamic rebound spikes from excitation-driven spikes, they might read out synchronous activity that only occurs for rebound spikes. Thereby, only coordinated activity in

different thalamocortical neurons may lead to movement initiation [45] or muscle contraction [18]. Similarly, in mice optical stimulation of neurons in a BG output region induces different muscular responses from a single twitch to tremor-like activity and continuous contraction with increasing stimulation frequency via rebound spikes [18]. Therefore, rebound activity in an individual Mthal neuron may not lead to muscle contraction, but instead coordinated rebound activity in several Mthal neurons may be required.

Impact of sensory responses on the transmission of motor signals

SNr neurons that decrease their activity during movement also respond to salient sensory stimuli such as auditory "Go" stimuli cueing movement [11, 27]. One proposed functional role for this brief firing rate increase is to prevent impulsive or premature responses during movement preparation in SNr neurons [11]. In addition, in our model we observed that, depending on the precise timing, sensory responses may also promote thalamocortical rebound spikes and movement. This effect was present when the sensory responses preceded the movement-related decrease by up to 40 ms (Figure 4).

In rats performing a stop-signal task the same SNr neurons responded to the "Go" stimulus also responded to an auditory "Stop" signal, which prompted the cancellation of the upcoming movement [11]. These responses were observed in trials, in which the rats correctly cancelled the movement, but not in trials where they failed to cancel the movement. These SNr responses to the "Stop" signal may delay movement initiation allowing another slower process to completely cancel the planned movement [41]. In line with this "pause-then-cancel" model of stopping [46], we observed that the SNr sensory responses can also prevent rebound spikes when they occur close to the time of the motor signal. In our model this suppression effect was present up to 40 ms after the onset of the movement-related decrease in SNr activity (Figure 4). Thereby, our model provides a prediction for the temporal window of the functional contribution of sensory responses in SNr to behaviour. Importantly, sensory responses can either promote or suppress movements, depending on their relative timing to the motor signal, providing a highly flexible means to integrate sensory and motor signals in nigrothalamic circuits.

Effects of deep brain stimulation

Our model points to the role of correlated BG activity in increasing rebound spikes in thalamocortical neurons. In particular, higher-order correlations lead to pauses in the SNr population activity promoting rebound spikes, while pairwise correlations alone did not affect the nigrothalamic transmission of motor signals (Figure 2B). This suggests that in Parkinson's disease higher-order correlations are relevant for motor symptoms, which offers some insight into the potential mechanisms by which deep-brain stimulation (DBS) might alleviate some of the motor symptoms such as rigidity and tremor. DBS in the STN and GPi has complex and diverse effects on the firing rate of neurons in SNr/GPi [47, 48] and thalamus [49]. According to our model strong increases in SNr and GPi firing rates observed after STN DBS [50, 51], would decrease the duration of the spontaneous pauses in the population activity (Figure 3C). Thereby, even for correlated SNr activity, the duration of the pauses would not be long enough to allow the generation of a rebound spike in the thalamocortical neuron.

Integration of decision making systems

In our model the generation of a rebound spike in thalamocortical neurons was strongly affected by single excitatory cortical input spikes (Figure 5). This means that the

transmission of a BG motor signal could be prevented by a single, precisely-timed cortical spike preceding the SNr movement-related decrease by up to 20 ms (Figure 5C). This indicates a powerful mechanism by which cortex could affect BG motor output signals. It has previously been argued that different decision making systems, incorporating different strategies, might co-exist in the brain [3, 52] and that the thalamus might be a key site for their integration [53]. Our model offers a potential mechanism by which conflicts between different decision-making systems could be resolved. In this case the precisely-timed cortical excitation would allow the cancellation of a BG motor signal. Furthermore, it is possible that thalamocortical neurons integrate habitual and goal-directed decision systems [52, 54], and that cancellation of BG motor signals serves as a means to prevent conflicting responses. Finally, the same mechanism for cancelling BG motor signals could also be used to exert cognitive control to overcome a habitual response. While this remains somewhat speculative at this point, our model provides a clear description of the inhibitory and excitatory inputs that would enable the modulation of a BG motor signal in thalamocortical neurons.

Acknowledgments

We would like to thank David Bilkey, Alejandro Jimenez, Lars Hunger, Amin Mirzaei, and Genela Morris for helpful discussions.

References

1. Albin RL, Young AB, Penney JB. The functional anatomy of basal ganglia disorders. Trends in neurosciences. 1989;12(10):366–375.

2. Alexander GE, Crutcher MD. Neural representations of the target (goal) of visually guided arm movements in three motor areas of the monkey. Journal of neurophysiology. 1990;64(1):164–178.

3. Redgrave P, Prescott TJ, Gurney K. The basal ganglia: a vertebrate solution to the selection problem? Neuroscience. 1999;89(4):1009–1023.

4. Hikosaka O, Takikawa Y, Kawagoe R. Role of the basal ganglia in the control of purposive saccadic eye movements. Physiological reviews. 2000;80(3):953–978.

5. Alexander GE, Crutcher MD. Functional architecture of basal ganglia circuits: neural substrates of parallel processing. Trends in neurosciences. 1990;13(7):266–271.

6. Wichmann T, DeLong MR. Functional and pathophysiological models of the basal ganglia. Current opinion in neurobiology. 1996;6(6):751–758.

7. Deniau J, Chevalier G. Disinhibition as a basic process in the expression of striatal functions. II. The striato-nigral influence on thalamocortical cells of the ventromedial thalamic nucleus. Brain research. 1985;334(2):227–233.

8. Hikosaka O, Wurtz RH. Visual and oculomotor functions of monkey substantia nigra pars reticulata. IV. Relation of substantia nigra to superior colliculus. Journal of neurophysiology. 1983;49(5):1285–1301.

9. Schultz W. Activity of pars reticulata neurons of monkey substantia nigra in relation to motor, sensory, and complex events. Journal of Neurophysiology. 1986;55(4):660–677.

10. Leblois A, Meissner W, Bioulac B, Gross CE, Hansel D, Boraud T. Late emergence of synchronized oscillatory activity in the pallidum during progressive Parkinsonism. European Journal of Neuroscience. 2007;26(6):1701–1713.

11. Schmidt R, Leventhal DK, Mallet N, Chen F, Berke JD. Canceling actions involves a race between basal ganglia pathways. Nature neuroscience. 2013;16(8):1118.

12. Bosch-Bouju C, Hyland BI, Parr-Brownlie LC. Motor thalamus integration of cortical, cerebellar and basal ganglia information: implications for normal and parkinsonian conditions. Frontiers in computational neuroscience. 2013;7:163.

13. Goldberg JH, Farries MA, Fee MS. Basal ganglia output to the thalamus: still a paradox. Trends in neurosciences. 2013;36(12):695–705.

14. Llinás R, Jahnsen H. Electrophysiology of mammalian thalamic neurones in vitro. Nature. 1982;297(5865):406.

15. Person AL, Perkel DJ. Unitary IPSPs drive precise thalamic spiking in a circuit required for learning. Neuron. 2005;46(1):129–140.

16. Person AL, Perkel DJ. Pallidal neuron activity increases during sensory relay through thalamus in a songbird circuit essential for learning. Journal of Neuroscience. 2007;27(32):8687–8698.

17. Leblois A, Bodor ÁL, Person AL, Perkel DJ. Millisecond timescale disinhibition mediates fast information transmission through an avian basal ganglia loop. Journal of Neuroscience. 2009;29(49):15420–15433.

18. Kim J, Kim Y, Nakajima R, Shin A, Jeong M, Park AH, et al. Inhibitory basal ganglia inputs induce excitatory motor signals in the thalamus. Neuron. 2017;95(5):1181–1196.

19. Kojima S, Doupe AJ. Activity propagation in an avian basal ganglia-thalamocortical circuit essential for vocal learning. Journal of Neuroscience. 2009;29(15):4782–4793.

20. Bosch-Bouju C, Smither RA, Hyland BI, Parr-Brownlie LC. Reduced reach-related modulation of motor thalamus neural activity in a rat model of Parkinson's disease. Journal of Neuroscience. 2014;34(48):15836–15850.

21. Edgerton JR, Jaeger D. Optogenetic activation of nigral inhibitory inputs to motor thalamus in the mouse reveals classic inhibition with little potential for rebound activation. Frontiers in Cellular Neuroscience. 2014;8:36.

22. Goldberg JH, Fee MS. A cortical motor nucleus drives the basal ganglia-recipient thalamus in singing birds. Nature neuroscience. 2012;15(4):620–627.

23. Goldberg JH, Farries MA, Fee MS. Integration of cortical and pallidal inputs in the basal ganglia-recipient thalamus of singing birds. Journal of neurophysiology. 2012;108(5):1403–1429.

24. Wilson CJ. Active decorrelation in the basal ganglia. Neuroscience. 2013;250:467–482.

25. Bar-Gad I, Heimer G, Ritov Y, Bergman H. Functional correlations between neighboring neurons in the primate globus pallidus are weak or nonexistent. Journal of Neuroscience. 2003;23(10):4012–4016.

26. Bergman H, Feingold A, Nini A, Raz A, Slovin H, Abeles M, et al. Physiological aspects of information processing in the basal ganglia of normal and parkinsonian primates. Trends in neurosciences. 1998;21(1):32–38.

27. Pan WX, Brown J, Dudman JT. Neural signals of extinction in the inhibitory microcircuit of the ventral midbrain. Nature neuroscience. 2013;16(1):71.

28. Rubin JE, Terman D. High frequency stimulation of the subthalamic nucleus eliminates pathological thalamic rhythmicity in a computational model. Journal of computational neuroscience. 2004;16(3):211–235.

29. Rinzel J. Excitation dynamics: insights from simplified membrane models. In: Fed. Proc. vol. 44; 1985. p. 2944–2946.

30. Gerstner W, Kistler WM. Spiking neuron models: Single neurons, populations, plasticity. Cambridge university press; 2002.

31. Kase D, Uta D, Ishihara H, Imoto K. Inhibitory synaptic transmission from the substantia nigra pars reticulata to the ventral medial thalamus in mice. Neuroscience research. 2015;97:26–35.

32. Ermentrout GB, Terman DH. Mathematical foundations of neuroscience. vol. 35. Springer Science & Business Media; 2010.

33. Staude B, Grün S, Rotter S. Higher-order correlations and cumulants. In: Analysis of parallel spike trains. Springer; 2010. p. 253–280.

34. Bujan AF, Aertsen A, Kumar A. Role of input correlations in shaping the variability and noise correlations of evoked activity in the neocortex. Journal of Neuroscience. 2015;35(22):8611–8625.

35. Kuhn A, Aertsen A, Rotter S. Higher-order statistics of input ensembles and the response of simple model neurons. Neural Computation. 2003;15(1):67–101.

36. Lindahl M, Kotaleski JH. Untangling basal ganglia network dynamics and function–role of dopamine depletion and inhibition investigated in a spiking network model. eneuro. 2016; p. ENEURO–0156.

37. Brown P, Oliviero A, Mazzone P, Insola A, Tonali P, Di Lazzaro V. Dopamine dependency of oscillations between subthalamic nucleus and pallidum in Parkinson's disease. Journal of Neuroscience. 2001;21(3):1033–1038.

38. Avila I, Parr-Brownlie LC, Brazhnik E, Castañeda E, Bergstrom DA, Walters JR. Beta frequency synchronization in basal ganglia output during rest and walk in a hemiparkinsonian rat. Experimental neurology. 2010;221(2):307–319.

39. Mirzaei A, Kumar A, Leventhal D, Mallet N, Aertsen A, Berke J, et al. Sensorimotor processing in the basal ganglia leads to transient beta oscillations during behavior. Journal of Neuroscience. 2017;37(46):1289–17.

40. Magnin M, Morel A, Jeanmonod D. Single-unit analysis of the pallidum, thalamus and subthalamic nucleus in parkinsonian patients. Neuroscience. 2000;96(3):549–564.

41. Mallet N, Schmidt R, Leventhal D, Chen F, Amer N, Boraud T, et al. Arkypallidal cells send a stop signal to striatum. Neuron. 2016;89(2):308–316.

42. Saito Y, Isa T. Electrophysiological and morphological properties of neurons in the rat superior colliculus. I. Neurons in the intermediate layer. Journal of neurophysiology. 1999;82(2):754–767.

43. Wilson CJ. Oscillators and oscillations in the basal ganglia. The Neuroscientist. 2015;21(5):530–539.

44. Nevado-Holgado AJ, Mallet N, Magill PJ, Bogacz R. Effective connectivity of the subthalamic nucleus–globus pallidus network during Parkinsonian oscillations. The Journal of physiology. 2014;592(7):1429–1455.

45. Gaidica M, Hurst A, Cyr C, Leventhal DK. Distinct Populations of Motor Thalamic Neurons Encode Action Initiation, Action Selection, and Movement Vigor. Journal of Neuroscience. 2018;doi:10.1523/JNEUROSCI.0463-18.2018.

46. Schmidt R, Berke JD. A Pause-then-Cancel model of stopping: evidence from basal ganglia neurophysiology. Phil Trans R Soc B. 2017;372(1718):20160202.

47. Bar-Gad I, Elias S, Vaadia E, Bergman H. Complex locking rather than complete cessation of neuronal activity in the globus pallidus of a 1-methyl-4-phenyl-1, 2, 3, 6-tetrahydropyridine-treated primate in response to pallidal microstimulation. Journal of Neuroscience. 2004;24(33):7410–7419.

48. Zimnik AJ, Nora GJ, Desmurget M, Turner RS. Movement-related discharge in the macaque globus pallidus during high-frequency stimulation of the subthalamic nucleus. Journal of Neuroscience. 2015;35(9):3978–3989.

49. Muralidharan A, Zhang J, Ghosh D, Johnson MD, Baker KB, Vitek JL. Modulation of Neuronal Activity in the Motor Thalamus during GPi-DBS in the MPTP Nonhuman Primate Model of Parkinson's Disease. Brain stimulation. 2017;10(1):126–138.

50. Hashimoto T, Elder CM, Okun MS, Patrick SK, Vitek JL. Stimulation of the subthalamic nucleus changes the firing pattern of pallidal neurons. Journal of neuroscience. 2003;23(5):1916–1923.

51. Maurice N, Thierry AM, Glowinski J, Deniau JM. Spontaneous and evoked activity of substantia nigra pars reticulata neurons during high-frequency stimulation of the subthalamic nucleus. Journal of Neuroscience. 2003;23(30):9929–9936.

52. Daw ND, Niv Y, Dayan P. Uncertainty-based competition between prefrontal and dorsolateral striatal systems for behavioral control. Nature neuroscience. 2005;8(12):1704.

53. Haber SN, Calzavara R. The cortico-basal ganglia integrative network: the role of the thalamus. Brain research bulletin. 2009;78(2-3):69–74.

54. Redgrave P, Rodriguez M, Smith Y, Rodriguez-Oroz MC, Lehericy S, Bergman H, et al. Goal-directed and habitual control in the basal ganglia: implications for Parkinson's disease. Nature Reviews Neuroscience. 2010;11(11):760.